Hindawi
Advances in Civil Engineering
Volume 2023, Article ID 5591853, 13 pages
https://doi.org/10.1155/2023/5591853

Research Article

A Novel Method of Self-Healing Concrete to Improve Durability and Extend the Service Life of Civil Infrastructure

Yan Xue, Weiliang Gao, and Yanming Zhao

School of Transportation Engineering, Huanghe Jiaotong University, Jiaozuo, Henan 454000, China

Correspondence should be addressed to Yan Xue; 2019081004@zjtu.edu.cn

Received 10 May 2023; Revised 4 August 2023; Accepted 10 August 2023; Published 26 August 2023

Academic Editor: Rahul Biswas

Concrete civil infrastructure often suffers severe damage to its internal structure due to insufficient durability in high and cold complex environments, affecting the service life of the infrastructure. Therefore, a novel method based on nanofillers for self-healing concrete is proposed to optimize the durability mix proportion of high-performance concrete in complex high and cold environments, which improves the strength recovery rate of concrete. Moreover, a concrete durability prediction model based on particle swarm optimization-least squares support vector machine (PSO-LSSVM) and improved NSGA-II (nondominated sorting genetic algorithm II) algorithm was proposed to quickly and accurately determine the optimization scheme of self-healing concrete mix proportion. First, the model employs PSO-LSSVM to achieve highly accurate predictions of relative dynamic elastic modulus and chloride ion permeability coefficient, which are key indicators of the concrete durability. Subsequently, the predicted regression functions for concrete durability are utilized as fitness functions, and the improved NSGA-II algorithm is employed to obtain the optimal mix ratio for durable concrete. Finally, the Pareto frontier solution set is processed using the ideal point method selection approach to determine the optimal concrete mix ratio scheme. To assess the self-healing ability of the proposed concrete, a concrete durability test study is conducted. Experimental research shows that the durability of the proposed self-healing concrete has been significantly improved. The optimized PSO-LSSVM model demonstrates excellent generalization capability. The coefficient of determination between the predicted and actual values in the test dataset is 0.9357, and the root-mean-square error is 0.10267. Building upon this, the enhanced concrete durability prediction model based on the NSGA-II algorithm proves to be highly effective in predicting the optimal concrete mix proportion scheme. The predicted values of chloride ion permeability coefficient and relative dynamic elastic modulus of the proposed model differ from the actual experimental values by 1.29% and 0.59%, significantly better than the other prediction models.

1. Introduction

Under the combined effect of load, deformation, and environmental factors, concrete may experience tensile stress that exceeds its tensile strength, resulting in cracking [1]. Concrete cracking is a challenging issue to prevent, as cracks provide pathways for the ingress of water, carbon dioxide, oxygen, chlorides, and sulfates from the surrounding environment. This ingress further deteriorates the safety and durability of concrete structures, leading to a vicious cycle of "concrete deterioration → concrete cracking → erosion by harmful substances → further deterioration". Ultimately, this cycle negatively impacts the safety, durability, and service life of reinforced concrete structures [2, 3].

Self-healing concrete can repair cracks generated by concrete because of its self-healing nature is a current research hot spot [4, 5]. Self-healing concrete mimics the function of biological tissue damage healing by compounding special components in the traditional components of concrete to form an intelligent self-healing system inside it, which automatically triggers a repair response to heal when cracks or damage occurs in the concrete material [6]. The self-healing of concrete can be categorized into natural healing and engineered healing [7]. Natural healing is an inherent phenomenon in concrete, where small to medium-sized cracks that occur in the concrete structure are healed through the hydration reaction of previously unhydrated cement particles with water and carbon dioxide [8]. The disadvantage of natural

healing is that it takes too long to act and is not applicable to some concrete structures with large crack widths. Engineering self-healing is a technical measure that artificially enhances the self-healing ability of concrete through the medium of fibrous materials, microorganisms, and capsules [9]. Compared to conventional self-healing techniques, the incorporation of the nanofillers improves the spatial network structure of concrete and controls the morphology of hydration products at the microscale. In addition, the nanofillers also improve the spatial distribution of concrete cracks [10]. It has been shown that nucleation effect, water absorption effect, and very good filling effect of nanofillers. Therefore, when appropriate amounts of nanofillers are incorporated into concrete, the nanoparticles can fill the pores inside the concrete and improve its compactness, which in turn improves the concrete strength. However, the research results of self-healing concrete based on nanofillers are relatively few [11]. A new method of self-healing concrete based on nanofillers is proposed for improving the durability and extending the service life of the civil infrastructure.

The durability of concrete is closely related to the mix ratio of raw materials, and scholars at home and abroad have been conducting extensive research on the durability of concrete and the optimization of the mix ratio of raw materials. Geng et al. [12] conducted experimental research on the early strength of prefabricated silica fume concrete. Cao et al. [13] optimized the mix proportion of high-strength and high-performance concrete. The traditional experimental methods for predicting the durability and strength of concrete, as well as optimizing the mix ratio, have many limitations and low efficiency. With the development of computer technology and the popularization of machine learning algorithms, a new approach has been provided for studying the durability and strength prediction of concrete, as well as the optimization of mix proportions. Tu et al. [14] used the Genetic Algorithms Back-Propagation optimized neural network model to predict the impermeability performance of concrete. Wu [15] and Abunassar et al. [16] used radial basis funtion-artificial neural network (ANN) and support vector machine (SVM)-ANN network models to predict and analyze the compressive strength performance of concrete, respectively. The above research used machine learning algorithms to predict and analyze the impermeability and strength of concrete, but rarely combined concrete performance prediction with mix ratio optimization. The constructed model considers fewer influencing factors during the prediction and has a relatively single objective during optimization.

Therefore, aiming at the problems of considering fewer influencing factors and a single optimization objective in the prediction model, the article selects the dual objectives of frost resistance and permeability resistance as the main indicators of concrete durability, and constructs an evaluation model based on particle swarm optimization-least squares support vector machine (PSO-LSSVM) and improved nondominated sorting genetic algorithm II (NSGA-II) algorithm to quickly and accurately determine the mix proportion optimization plan. As an intelligent algorithm, LSSVM can effectively overcome nonlinear problems. The algorithm is global and suitable for small sample data. Regarding the regularization parameter C and the kernel function width parameter σ, which significantly influence the classification and recognition performance of the LSSVM model, we acknowledge the concern about random settings potentially leading to the suboptimal solutions. To address this issue, we have introduced the PSO algorithm to enhance the LSSVM model [17–19]. This optimization technique aims to find better solutions and improve the classification and recognition accuracy of the model, ensuring that it meets the required performance standards. The NSGA-II algorithm is one of the most popular multiobjective genetic algorithms, which can effectively handle multiobjective optimization problems and has the advantages of fast running speed and good convergence of the solution set. To explore the self-healing ability of new self-healing concrete, this article conducted durability experiments to explore the trend of the influence of the content and type of nanofillers on the self-healing performance of the concrete. In order to obtain the optimal combination of concrete mix ratio parameters and reduce the resource consumption of manpower, material resources, and time in the design of mix ratio schemes, this article combines intelligent algorithms with mix ratio design to achieve intelligent and precise concrete mix ratio design, which has a certain guiding role for engineering practice, especially for high-performance concrete mix ratio optimization in alpine complex environment.

The innovation of this article is as follows:

(1) A novel method of self-healing concrete based on nanofillers has been proposed to extend the service life of civil infrastructure.

(2) An evaluation model based on PSO-LSSVM and improved NSGA-II algorithm has been constructed to evaluate the durability of self-healing concrete.

(3) To solve the problem of traditional NSGA-II falling into local optimization, an improved NSGA-II algorithm is proposed, which introduces a Tent chaotic map to initialize the population and adopts an adaptive crossover operator to avoid the algorithm falling into local optimization.

2. Research Significance

Concrete mix design is a complex process that traditionally relies on extensive knowledge and experience in the concrete technology. Currently, obtaining concrete mix proportions that meet specific requirements still involves a significant amount of trial and error and relies heavily on the experience. This trial mixing approach consumes considerable manpower, material resources, and time. With the rapid development of artificial intelligence technology in the 21st century, it has found widespread applications in various research domains. Intelligent algorithms offer remarkable adaptability and fitting capability, making them well-suited for predicting the concrete properties accurately. In this study, we propose a concrete mix proportion optimization model based on the intelligent algorithms. By integrating intelligent algorithms with mix proportion design and utilizing a vast amount of mix proportion data, we can simulate

and optimize the concrete mix proportion design. As a result, the resource consumption of manpower, material resources, and time in the trial mixing process is significantly reduced. This not only saves costs but also achieves an intelligent and precise concrete mix proportion design.

3. State of the Art

3.1. Nano Self-Healing Concrete. Currently, one of the common methods to improve the performance of concrete is the compounding of materials. The nanomaterials incorporated into concrete can improve and enhance the physical and mechanical properties of concrete to a certain extent [20].

Abousnina et al. [21] used nanoparticles for self-healing cement paste first. Stefanidou et al. [22] incorporated nano-SiO_2 into concrete to verify the feasibility of self-healing of nanoconcrete. Stefanidou et al. [23] found that the addition of nanoparticles to cement slurry facilitated the healing of cement slurry and accelerated the healing rate in water. Gohar et al. [24] and Rajasegar and Kumaar [25] found that silica nanoparticles increased the strength of concrete. Evangelia and Maria [26] found that the addition of calcium oxide nanoparticles reduced the water penetration through cracks and increased the self-healing efficiency.

3.2. Self-Healing Concrete Ratio Optimization. Concrete durability is the main factor that determines the service life of concrete. In recent years, in the actual project because of the lack of concrete durability and structural damage has occurred repeatedly, bringing huge loss of life and property. The early durability of concrete is mainly determined by the concrete ratio. Therefore, it is important to study the ratio of concrete to service life of concrete.

At present, researchers have conducted some studies on concrete impermeability and ratio optimization. Wang et al. [27] investigated the early strength and durability performance of concrete under the effect of multiple factors based on orthogonal tests for freeze–thaw environment. He et al. [28] investigated the mechanism of highland environmental influence on the strength and permeability of concrete. Guo et al. [29] optimized the concrete mix ratio design by simulation test based on the crack resistance performance of bridge deck slab concrete in alpine region. Gong et al. [30] optimized the mix ratio of C50 concrete for island concrete engineering. Leite and Santana [31], based on the analysis of concrete material combination mixing effect, the optimization of the mix ratio design for high-performance concrete was achieved. Xu et al. [32] optimized the mix ratio of precast concrete from the perspective of precast concrete and through orthogonal tests. The above research adopts traditional experimental methods to study the impermeability of concrete and optimize the mix ratio, which is not only time-consuming and labor-intensive, but also the obtained optimal mix ratio is not accurate enough. With the development and application of machine learning algorithms, some scholars began to try to solve the objective optimization problem by machine learning algorithms. Zhang et al. [33] successfully obtained the dual-objective mix ratio optimization problem and Pareto frontier for high-performance concrete using a multiobjective optimization model, and used machine learning and random forest methods to optimize the solution. Huang et al. [34] established a new Firefly algorithm SVR model, which makes the optimization of steel fiber concrete mix ratio more refined. Xue [35] used PSO-LSSVM model to predict the compressive strength of concrete, and verified the reliability of the model. Han et al. [36] put forward a multi-objective optimization model of wet-sprayed concrete mixture ratio parameters based on BP-NSGAII to obtain the optimal design scheme of wet-sprayed concrete parameters. Taking BP neural network as fitness function, the improved NSGA-II method is used to find Pareto optimal solution of decision variables in fitness function, so as to obtain the best wet sprayed concrete parameters. In order to achieve fast and accurate determination of the mix optimization scheme, Liu et al. [37] proposed a hybrid intelligent prediction model integrating random forest and LSSVM algorithms for predicting the permeability of concrete. On this basis, Liu et al. [38], Wu et al. [39], and Chen et al. [40] introduced the double objectives of frost resistance and impermeability as durability evaluation indicators, and, respectively, adopted SVM-NSGA-II algorithm, random forest-NSGA-II algorithm and LSSVM-NSGA-II algorithm for multiobjective optimization to obtain the optimal concrete mix proportion scheme.

4. Methodology

4.1. PSO-LSSVM Model

4.1.1. Least Squares Support Vector Machines. The basic principle of the mathematical model of the LSSVM algorithm is as follows: assume that the training sample set $D = \{(x_i, y_i), i = 1, 2, \ldots, n\}$. Then the regression function at this point is

$$y_i = \omega\varphi(x_i) + b, \tag{1}$$

where y_i denotes the i-th predicted value with d-dimension, x_i denotes the i-th input vector with d-dimension, ω is the weight vector of the regression function, and b is the bias.

Unlike SVMs, LSSVM utilizes the error in the optimization objective ξ_i squared as the loss function of its model. Also, by converting the constraints into formula constraints, its optimization problem becomes:

$$\begin{aligned} &\min \frac{1}{2} \| \omega\|^2 + u\frac{1}{2}\sum_{i=1}^{n} \boldsymbol{e}_i^2 \\ &\text{st.}\omega\varphi(x_i) + b + \boldsymbol{e}_i = y_i, \end{aligned} \tag{2}$$

where c is the regularization parameter and e_i is the error vector. Lagrangian function is established to solve the above problem, i.e.,

$$L(\omega, b, \boldsymbol{e}, \xi) = \frac{1}{2} \| \omega\|^2 + u\frac{1}{2}\sum_{i=1}^{n} \boldsymbol{e}_i^2 - \sum_{i=1}^{n} \xi_i[\omega\varphi(x_i) + b + \boldsymbol{e}_i - y_i]. \tag{3}$$

The optimal solution satisfies the Karush–Kuhn–Tucker (KKT) optimization condition. The ω, b, e, ξ in Formula (3) are calculated as the partial derivative, and then make them

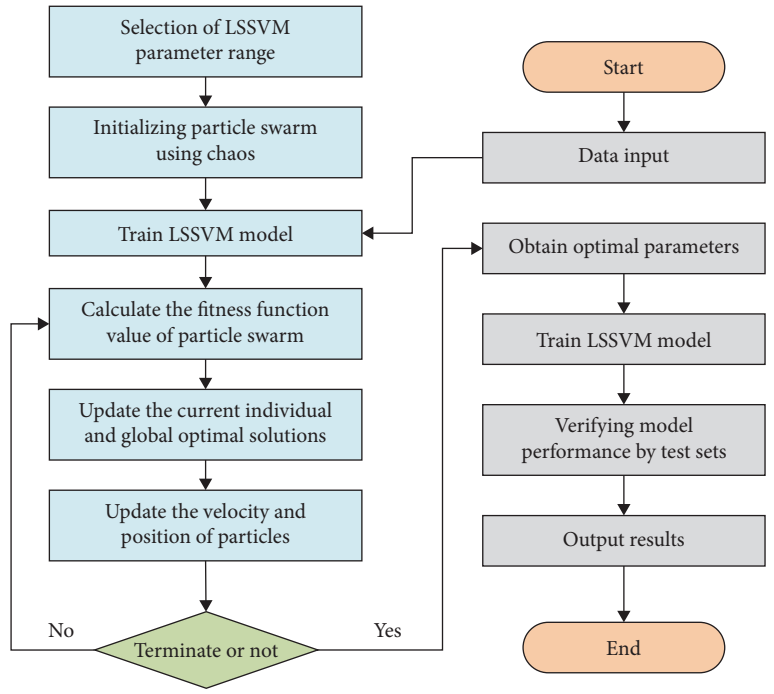

Figure 1: PSO-LSSVM flowchart.

equal to zero.

$$\begin{cases} \dfrac{\partial L}{\partial \omega} = 0 \rightarrow \omega = \sum_{i=1}^{n} \xi \phi(x_i) \\ \dfrac{\partial L}{\partial b} = 0 \rightarrow \sum_{i=1}^{n} \xi_i = 0 \\ \dfrac{\partial L}{\partial e} = 0 \rightarrow \xi_i = u\boldsymbol{e}_i \\ \dfrac{\partial L}{\partial \xi} = 0 \rightarrow \omega\varphi(x_i) + b + \boldsymbol{e}_i - y_i = 0. \end{cases} \tag{4}$$

The elimination of the variables ω and e after the homogeneous solution transformation of the above conditions yields b and ξ the optimal solution matrix.

$$\begin{bmatrix} 0 \\ \boldsymbol{Y} \end{bmatrix} = \begin{bmatrix} 0 & \boldsymbol{Z}^T \\ \boldsymbol{Z} & \boldsymbol{K} + c^{-1}\boldsymbol{E} \end{bmatrix} \begin{bmatrix} b \\ \xi \end{bmatrix}, \tag{5}$$

where $\xi = [\xi_1, \xi_2, \ldots, \xi_n]^{\mathrm{T}}$ is the Lagrange multiplier. $Z = [1, 1, \ldots, 1]^{\mathrm{T}}$ and $y = [y_1, y_2, \ldots, y_n]^{\mathrm{T}}$. e is the unit matrix of order n and k denotes the kernel function matrix defined by

$$\boldsymbol{K} = K(x_i, x_j) = \varphi(x_i)\varphi(x_j). \tag{6}$$

The LSSVM decision function is expressed as follows:

$$y(x) = \sum_{i=1}^{n} \xi_i K(x, x_i) + b, \tag{7}$$

$$K(x, x_i) = \exp\left(-\frac{\|x - x_i\|^2}{2\sigma^2}\right), \tag{8}$$

where σ^2 denotes the width parameter and x denotes the output variable.

4.1.2. Parameter Preferences. The choice of LSSVM parameters determines the performance of the model prediction. The width parameter σ^2 and the regularization parameter u of the Gaussian kernel function both have some influence on the prediction effect of LSSVM. In this paper, we choose the PSO algorithm to find the optimal combination of the regularization parameter u of LSSVM and the kernel width coefficient σ to build a prediction model based on PSO-LSSVM. The construction process of the model is shown in Figure 1.

The steps to construct the PSO-LSSVM-based model are as follows:

Step 1: Organize and collect samples, and preprocess the raw data.

Step 2: Particle swarm parameters initialization. Set the appropriate range of values for (c, σ), determine the number of particle swarms q, the maximum number of iterations $t_{\max}$, the learning factors c_1 and c_2, the inertia weight factors $\omega_{\max}$ and $\omega_{\min}$, and randomly generate the initial particle swarms.

Step 3: The parameter combinations generating different c and σ are input to the PSO-LSSVM model training, and the particle swarm fitness values for each generation are determined using the fitness function, and the root-mean-square error (RMSE) is chosen to evaluate the goodness of the function of particle fitness, as shown in Formula (9):

$$\mathrm{RMSE} = \frac{1}{n}\sqrt{\sum_{i=1}^{n}(y - y_i)^2}, \tag{9}$$

where y_i represents the predicted value of the sample, y represents the actual value, and n represents the number.

Step 4: The current fitness value $f(x_i)$ of each particle is compared with the fitness value $f(P_{\mathrm{best}})$ of the historical optimal position for analysis. If $f(x_i) \le f(P_{\mathrm{best}})$, then update $P_{\mathrm{bes}} = x_i$. Compare the magnitude of the fitness value $f(x_i)$ of the optimal position of each particle and the fitness value $f(G_{\mathrm{best}})$ of the optimal position of the whole particle population, if $f(x_i) \le f(P_{\mathrm{best}})$, then update $G_{\mathrm{bes}} = x_i$. Repeat the above operation until the optimal combination of solutions is obtained.

Step 5: Build PSO-LSSVM training model.

4.2. Improved NSGA-II Algorithm Implementation. The traditional NSGA-II has the problem of falling into local optimum. The improved NSGA-II algorithm is used for the optimization of mix parameters to determine the Pareto optimal solution set of the optimal mix parameters for both permeability and frost resistance of the concrete. To address the shortcomings of the traditional NSGA-II algorithm, the Tent chaotic mapping is introduced to initialize the population and adopts an adaptive crossover operator to avoid falling into a local optimum.

(1) Initialized population strategy based on Tent chaotic mapping

In the field of intelligent optimization, chaotic mappings are often used to initialize populations with better results than pseudorandom numbers. There are many chaotic mappings, among which Tent mapping is more convenient due to its simple structure and also it can produce uniformly distributed individuals. Therefore, in this paper, the Tent mapping is cited as an improved method for initializing the population of NSGA-II algorithm, whose expression is given by Formula (10).

$$x_{m+1} = f(x_m) = \begin{cases} \dfrac{x_m}{a}, & x_m \in [0, a) \\ \dfrac{1 - x_m}{1 - a}, & x_m \in [a, 1], \end{cases} \tag{10}$$

where $a = 0.499$. x_m denotes the m-th chaotic number.

(2) Adaptive crossover operator

The conventional NSGA-II uses analog binary crossover operator, which has a small moving space for crossover and is easy to fall into the local optimum. The normal distribution crossover operator and the arithmetic crossover operator are introduced. In the early iteration of the algorithm, the normal distribution crossover operator is used with greater probability to improve the search ability of the algorithm in the early stage and avoid falling into the local optimum. The arithmetic crossover operator is used in the later stage of the algorithm to reduce the search space and accelerate the convergence speed of the algorithm. The normal distribution crossover operator and the arithmetic crossover operator are given by Formulas (11) and (12).

$$x_{1,i}^{t+1}, x_{2,i}^{t+1} = \begin{cases} \dfrac{x_{1,i}^t + x_{2,i}^t}{2} \pm 1.481 \dfrac{x_{1,i}^t - x_{2,i}^t}{2} |N(0,1)|, & v \le 0.5 \\ \dfrac{x_{1,i}^t + x_{2,i}^t}{2} \mp 1.481 \dfrac{x_{1,i}^t - x_{2,i}^t}{2} |N(0,1)|, & v > 0.5 \end{cases} \tag{11}$$

$$\begin{aligned} x_{1,i}^{t+1} &= \lambda \times x_{1,i}^t + (1 - \lambda) \times x_{2,i}^t \\ x_{2,i}^{t+1} &= (1 - \lambda) \times x_{1,i}^t + \lambda \times x_{2,i}^t, \end{aligned} \tag{12}$$

where $x_{1,i}^{t+1}$ and $x_{2,i}^{t+1}$ denote the two individuals in the $t+1$-th generation of the i-th variable. $|N(0,1)|$ represents a random number subject to normal distribution, v denotes a random number between (0, 1), and λ denotes the variable associated with the dominance rank, whose expression is given by Formula (13).

$$\lambda = \frac{x_{2,i}^t \cdot \mathrm{rank}}{x_{1,i}^t \cdot \mathrm{rank} + x_{2,i}^t \cdot \mathrm{rank}}, \tag{13}$$

where rank denotes dominance rank.

The crossover operator selection factor is a variable related to the number of iterations and represents the probability of selecting a normally distributed crossover operator. Let it be $P(t)$, where t is the number of current evolutionary generations. Consider that more normally distributed crossover operators should be selected at the beginning of the algorithm and more arithmetic crossover operators at the end of the algorithm. Referring to the cooling mechanism of simulated annealing, the value of the crossover operator selection factor is dynamically adjusted by the annealing factor. The expression is given by Formula (14).

$$\begin{aligned} P(1) &= 1 \\ P(t+1) &= \beta \times P(t), \end{aligned} \tag{14}$$

where β denotes the annealing factor, which generally takes a value between 0.8 and 0.99.

The flowchart of the improved NSGA-II algorithm is shown in Figure 2.

5. Self-Healing Concrete Ratio Optimization Model

In real life, the relationship between concrete mix materials and durability is highly nonlinear. We propose a multiobjective optimization intelligent algorithm based on PSO-LSSVM and improved NSGA-II to optimize the fit ratio, replacing the traditional mathematical function with the SVM model as the fitness function in the multiobjective genetic algorithm. First, frost resistance and impermeability are used as durability evaluation indicators. The PSO-LSSVM model is used to learn the concrete mix ratio and obtain the nonlinear prediction

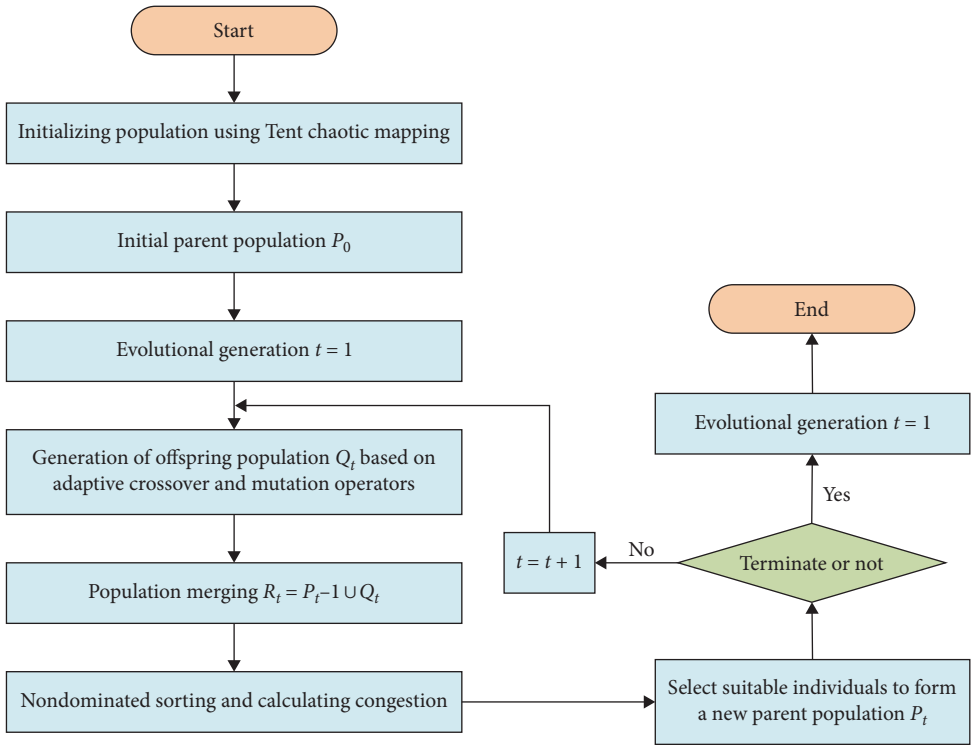

Figure 2: Flowchart of improved NSGA-II algorithm.

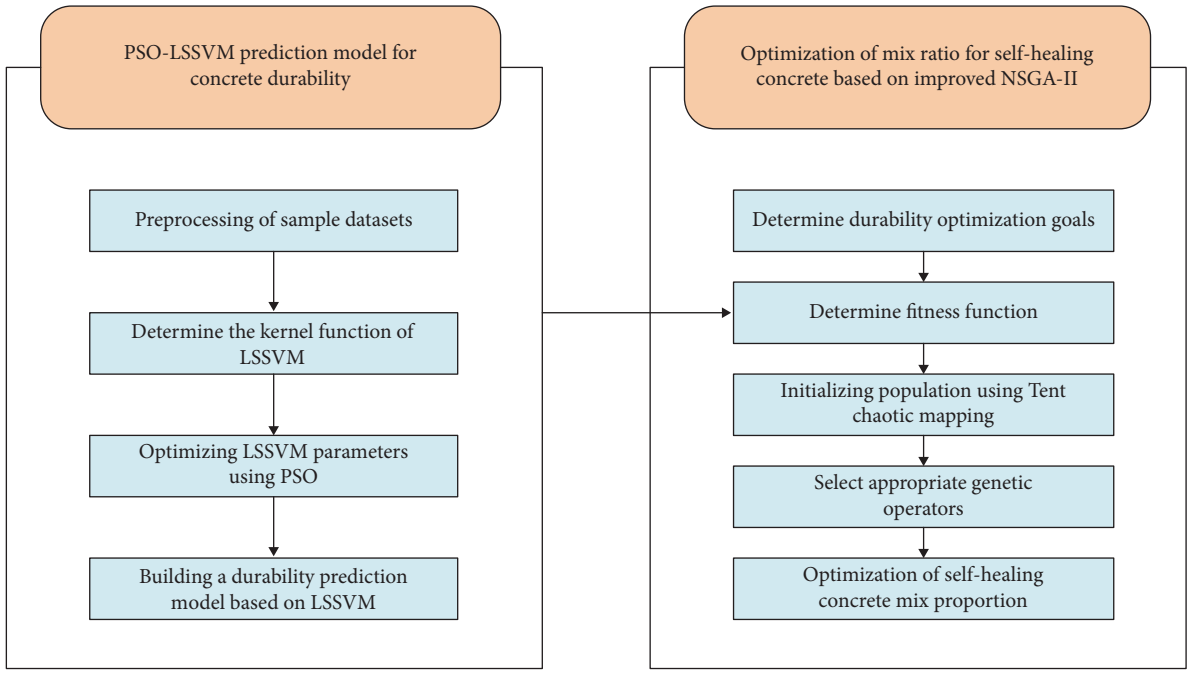

Figure 3: The flowchart of proposed method.

relationship between concrete durability and mix ratio. Then, the predictive regression function of the two indicators is taken as the fitness function of the improved NSGA-II algorithm. The Pareto frontier solution set determines the combination of concrete mix ratio parameters that meet both frost resistance and impermeability performance. Finally, the optimal concrete proportioning scheme is selected by the ideal point method. The flowchart of proposed method is shown in Figure 3.

5.1. Data Normalization Process. The optimization objective of this article is to obtain the optimal mix ratio of concrete that meets the conditions of frost resistance and impermeability durability. Ten factors, including water cement ratio,

sand ratio, fly ash, cement, fine aggregate, nanosilica, coarse aggregate, water reducing agent, expansion agent, and air entraining agent, are selected as input variables for the multiobjective genetic algorithm in the concrete mix proportion. The above 10 variables are represented as x_1, x_2, x_3, x_4, x_5, x_6, x_7, x_8, x_9, and x_{10}, respectively.

Different concrete ratio indexes have different scales, and some data in the sample are too large or too small will increase the burden of the algorithm in the training process, resulting in data overwhelm or network nonconvergence. Therefore, it is necessary to normalize the sample data. Data normalization can make the input data in a certain interval, such as (0, 1), (−1, 1) etc., which eliminates the influence of different sample eigenvalue dimensions on the prediction efficiency and accuracy. In this paper, we choose to normalize the sample input data to the interval (−1, 1).

5.2. Multiobjective Optimization

5.2.1. Construction Based on LSSVM Fitness Function. In the modified NSGA-II algorithm, there are two objective functions set, namely, the relative dynamic elastic modulus F and the chloride ion permeability coefficient θ. These two objective functions are output by the PSO–LSSVM-based concrete frost durability function. According to the experimental experience, $F \geq 85\%$ was set after 300 freeze–thaw cycles of concrete. To meet the good durability of concrete against permeability, the coefficient $\theta \leq 3.\ 5 \times 10^{-8}\,\mathrm{cm}^2/\mathrm{s}$ was set after 28 days.

The problem of complex nonlinear relationships between input variables and output targets, as well as the inability to provide specific function expressions, was solved—which using the PSO-LSSVM model. The SVM-based regression function is as follows.

$$\mathrm{svm}(X) = \sum_{i=1}^{10} (\alpha_i - \alpha_i^*) \exp\left(-\frac{\|x_i - x\|^2}{2\sigma^2}\right) + b, \tag{15}$$

where $X = (x_1, x_2, x_3, x_4, x_5, x_6, x_7, x_8, x_9, \text{and } x_{10})$, the α_i and α_i^* are Lagrangian multipliers.

Two objective functions are defined as follows:

$$F[\mathrm{svm}(X)] > 85\%, \tag{16}$$

$$\theta[\mathrm{svm}(X)] < 3.5 \times 10^{-8}\mathrm{cm}^2/\mathrm{s}. \tag{17}$$

5.2.2. Range of Indicator Limits. To make the generated scheme more reasonable and feasible, the indicator constraints are added. The general form of the constraints is as follows.

$$s_{\mathrm{il}} < x_i < s_{\mathrm{iu}}, \tag{18}$$

where s_{il} are the lower limits of the *i-th* input variable. s_{iu} are the upper limits.

5.2.3. Optimum Ratio Selection. The Pareto optimal solution set obtained by the improved NSGA-II algorithm is not a unique solution, but a set of solutions that match the Pareto optimal state decision variables. In the optimization of concrete durability ratio, the ideal optimal solution needs to be obtained. Therefore, this paper uses the ideal point method to obtain a compromise solution from the optimal solution set. The ideal point is a correspondence point consisting of the optimal value corresponding to the optimal value using each objective pair $E\left(\eta_{E_{\mathrm{point}}}, Z_{E_{\mathrm{point}}}\right)$. The ideal point is the point of correspondence between the optimal values of each objective pair. After finding the corresponding equilibrium points, the distance between each optimal solution and the ideal point in the Pareto optimal solution diagram is calculated by the formula.

$$U_n = \left[\left(\frac{\left(\eta_{\mathrm{Pareto}} - \eta_{E_{\mathrm{point}}}\right)}{\eta_{E_{\mathrm{point}}}}\right)^2 + \left(\frac{\left(Z_{\mathrm{Pareto}} - Z_{E\,\mathrm{point}}\right)}{Z_{E_{\mathrm{point}}}}\right)^2\right]^{1/2}, \tag{19}$$

where $(\eta_{\mathrm{Pareto}}, Z_{\mathrm{Pareto}})$ are the coordinates corresponding to the optimal Pareto front point. $\left(\eta_{E_{\mathrm{point}}}, Z_{E_{\mathrm{point}}}\right)$ are the coordinates corresponding to the ideal point.

By calculating the distance function (Formula (20)), it can be seen that the optimal point is the point with the minimum distance from the ideal point, therefore, the ideal point method can be used to determine the set of optimal solutions from the Pareto front solution set that makes the multiobjective function optimal.

$$U_{\mathrm{opt}} = \min(U_n). \tag{20}$$

6. Example Analysis

6.1. Raw Materials and Specimen Preparation. The raw materials used in this article include P.O42.5 grade ordinary Portland cement produced by China National Materials Anhui Cement Co., Ltd., with a density of 3,050 kg/m^3, a specific surface area of 332 m^2/kg, an initial setting time of 194 min, and a final setting time of 261 min. The fly ash is selected from Class F Grade I fly ash produced by Anhui United Power Generation Co., Ltd., with a density of 2280 kg/m^3, a fineness of 6.1%, and a loss on ignition of 2.95%. Fine aggregate is selected from Anhui medium sand fine aggregate, with a fineness modulus of 2.7. The coarse aggregate is selected from natural crushed stones with a continuous grading of 5–31.5 mm from Chaohu scattered soldiers, with small stones accounting for 20% and large stones accounting for 80%. The slag powder selected is Anhui Yangtze River slag powder with the specification model of S95. The expansion agent selected is UEA concrete expansion agent from Longsheng of Laiyang. The longitudinal limited expansion rate of the concrete at 15 days is >0.02%, and the longitudinal limited dry shrinkage rate at 180 days is <0.02%. The waterproof performance is good, reaching grade P12 or above. Nano-SiO_2 is selected from Hebei Keze Metal Co., Ltd. at 20 nm, with an average particle size purity of 99.9%, a specific

Table 1: Sample information of endurance test data.

Variable	Parameter	Value		
		Min	Max	Average
Water/binder ratio, x_1	Input	0.33	0.41	0.36
Sand radio, x_2%	Input	45	36	40
Cement content, x_3 (kg/m^3)	Input	327	379	352.59
Flyash content, x_4 (kg/m^3)	Input	44	89	68.58
Fine aggregate content, x_5 (kg/m^3)	Input	652	900	763.15
Nano-SiO_2 content, x_6 (kg/m^3)	Input	4.7	5.2	4.96
Coarse aggregate content, x_7 (kg/m^3)	Input	1,020	1,198	1104.52
Water reducer content, x_8 (kg/m^3)	Input	3	4.6	4.29
Air-entraining agent content, x_9 (%)	Input	0	0.848	0.33
Expansive agent content, x_{10} (kg/m^3)	Input	26	29	27.58
Chloride ion permeability coefficient (10^{-8} cm^2/s)	Output	3.05	3.26	3.15
Relative dynamic elastic modulus (%)	Output	87.11	93.48	90.32

surface area of 240 m^2/g, a volume density of 0.06 g/cm^3, and a density of 2.2–2.6g/cm^3. The PWR-S model of polycarboxylate high-performance water reducing agent from Wuhan Port Company is selected as the water reducing agent. The air entraining agent is selected from Toho, Japan.

The self-healing concrete proportions were developed according to the "Ordinary Concrete Proportioning Design Regulations" (JGJ 55-2011) and prepared according to the specific proportions in Table 1. A total of 71 sets of sample data were collected through accelerated laboratory tests. Among them, 56 sets of samples were randomly selected to form the training set, and the remaining 15 sets of samples were used as the test set, and the input and output feature indicators were normalized to the interval (−1,1) to avoid flooding the features of the input vector.

6.2. PSO-LSSVM Model Prediction. The experimental machine configuration is 64-bit Win10 operating system. The CPU is Intel Core i5-12400F and RAM is 64 GB. The GPU is trained with NVIDIA GeForce RTX 2080 Ti with 11 GB video memory. The training network is built in Python 3.9 using the Pytorch module.

6.2.1. PSO-LSSVM Model Training. The important parameters in the LSSVM prediction model to determine the effectiveness of the model's prediction, such as regularization parameters and function width parameters. The regularization parameter u in the LSSVM model determines the model tolerance for errors. Generally speaking, the larger the u, the better the classification result, but it is prone to overfitting, which leading to a decrease in the model generalization ability. The smaller the u, the greater the error tolerance of the model, but it is prone to underfitting. Therefore, the value of u sets the regularization parameter range to $u = (0.01, 5)$. Kernel width parameter σ^2 determines the distribution of the model after high-dimensional mapping of low-dimensional samples to the new feature space. When σ^2 value sets too small, the Gaussian distribution will only act near the support vector samples, and there is a possibility that the accuracy of the

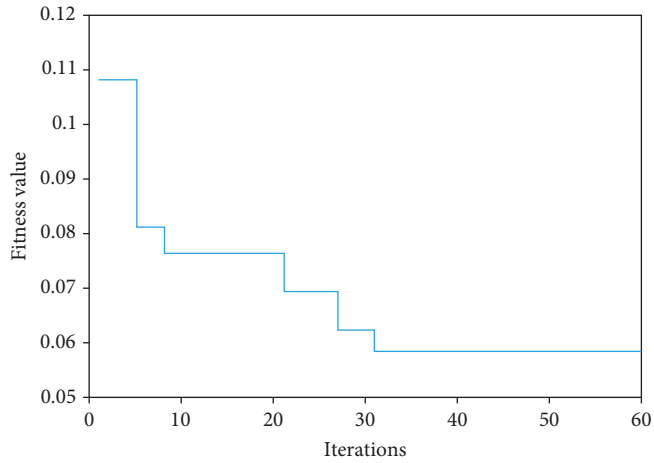

Figure 4: Optimal fitness curve in impermeability experiment.

training samples is high while the accuracy of the test samples is low, which means that overfitting occurs. When σ^2 value sets too large, the smoothing effect of the model will be too large, making it difficult to obtain high accuracy in the training set samples, thereby affecting the accuracy of the test set. Therefore, the value of σ^2 sets the kernel function width parameter range to $\sigma^2 = (0.05, 2)$.

The PSO parameters in this article are set as follows: maximum iteration number $k = 60$, population size $n = 30$, initial learning factor $c_1 = c_2 = 2$, initial inertia weight $w_1 = 0.8$, and termination inertia weight $w_2 = 0.5$. The PSO algorithm and fivefold cross-validation were used to optimize the width parameter σ^2 and regularization parameters u of the PSO-LSSVM prediction model for impermeability and frost resistance, respectively. About 56 sets of training set samples were input into the PSO-LSSVM model for the optimization processing. The iterative process of impermeability and frost resistance experiments is shown in Figures 4 and 5. In the impermeability experiment, it can be seen from the optimization curve in Figure 4 that the PSO-LSSVM model can

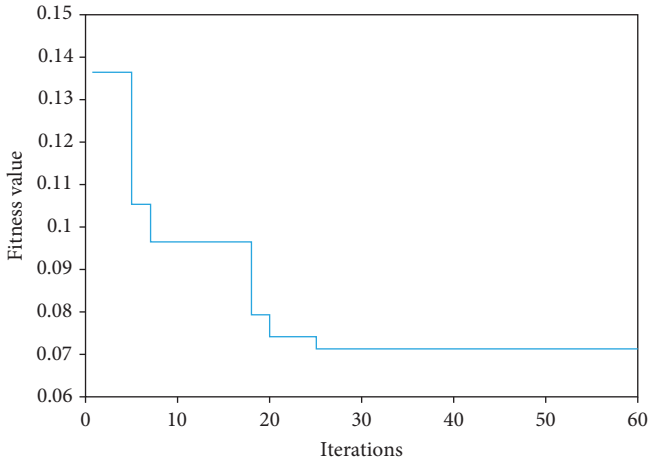

FIGURE 5: Optimal fitness curve in frost resistance experiment.

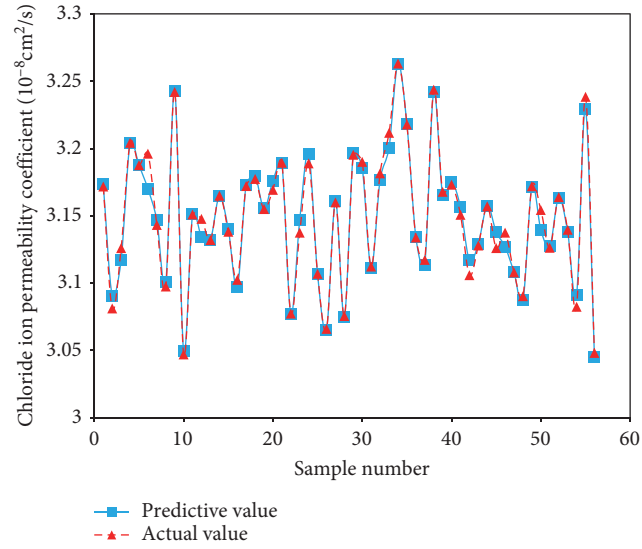

FIGURE 6: Predicted results of experimental training set for permeability resistance.

jump out of local optima multiple times and quickly obtain the global optimal solution. When the number of iterations reaches 32, the optimal applicability value stabilizes at 0.05861, and the population update is basically completed. After PSO optimization, when the inertia weight $w = 0.6493$ and the learning factor $c_1 = c_2 = 1.12$, the model parameters reach the optimal value, $u = 1.776$, $\sigma^2 = 0.1923$. Similarly, in the frost resistance experiment, it can be seen from the curve in Figure 5 that when the number of iterations reaches 26, the inertia weight of PSO algorithm $w = 0.6924$, and the learning factor $c_1 = c_2 = 1.36$, the optimal applicability value stabilizes at 0 07143, and the optimal model parameters are $u = 1.021$ and $\sigma^2 = 0.3988$.

6.2.2. Analysis of Forecast Results. In this paper, the PSO algorithm combined with fivefold cross-validation was used to optimize the width parameter σ^2 and the regularization parameter u for the PSO-LSSVM prediction models for frost resistance and permeability resistance, respectively. In order to quantify the prediction effect of PSO–LSSVM model, the coefficient of determination (R^2), RMSE, and mean absolute error (MAE) indexes are used to evaluate the prediction error. Below are the calculation Formulas (21)–(23) for three evaluation indicators.

The coefficient of determination (R^2) is defined as follows:

$$R^2 = \frac{\sum_{i=1}^{n} (d_i - d_{\text{mean}})^2 - \sum_{i=1}^{n} (d_i - y_i)^2}{\sum_{i=1}^{n} (d_i - d_{\text{mean}})^2}, \quad (21)$$

where y_i and d_i represent the i-th predicted value and the true value, respectively, n represents the total number of samples, and d_{mean} represents the average of the actual values.

The RMSE is defined as follows:

$$\text{RMSE} = \sqrt{\frac{1}{n} \sum_{i=1}^{n} (d_i - y_i)^2}. \quad (22)$$

The MAE is defined as follows:

$$\text{MAE} = \frac{1}{n} \sum_{i=1}^{n} |(y_i - d_i)|. \quad (23)$$

In the permeability resistance experiments, the model parameters were learned and optimized using the chloride permeability coefficient training set data, and the results are shown in Figure 6. From the figure, it can be seen that the PSO-LSSVM model can accurately express the decision law between the input and output. When the regularization parameter u is 1.776. The kernel function parameter σ^2 is 0.1923, the error between the predicted and actual values is minimized. After calculation, the R^2 between the actual value and the predicted value in the training set is 0.97933, RMSE is 0.05861, and MAE is 0.00125. The closer the R^2 is to 1, the closer the RMSE, and the MAE are to 0, which means that the better the performance of the prediction model is, and the closer the predicted value is to the actual value.

On this basis, the parameter-optimized model was used to process the test set data, as shown in Figure 7. It can be seen from the figure that the predicted values of the test set samples match very well with the experimental values. The coefficient of determination (R^2) between the actual value and the predicted value in the test set is 0.93575, the RMSE is 0.10267, and the MAE is 0.00511. The results show that the PSO-LSSVM prediction model can well reflect the nonlinear relationship between the raw material mix ratio and the chloride ion permeability coefficient, and has a good generalization ability.

Similarly, it can be seen from Figures 8 and 9 that the LSSVM prediction model can predict the relative dynamic elastic modulus very well. In the frost resistance experiments, the RMSE of the test results was minimized when the regularization parameter u was 1.021 and the kernel function

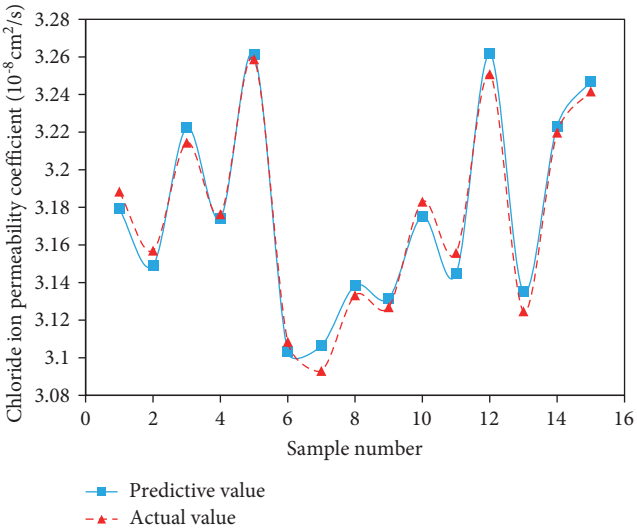

Figure 7: Predicted results of the experimental test set for permeability resistance.

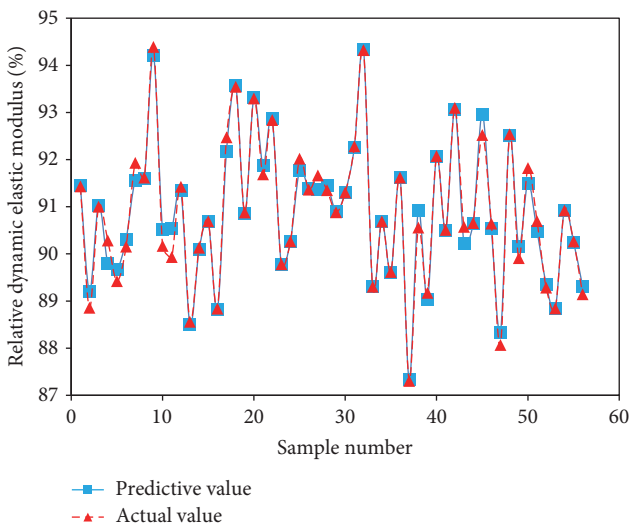

Figure 8: Prediction results of the training set of frost resistance experiment.

parameter σ^2 was 0.3988. The coefficient of determination (R^2) between the actual value and the predicted value in the training set is 0.98127, and the RMSE is 0.07143, the MAE is 0.00232. The coefficient of determination (R^2) between the actual value and the predicted value in the test set is 0.97792, and the RMSE is 0.09491, the MAE is 0.00458. The results showed that the optimized model had a very good agreement between the predicted values of the test set samples and the experimental values, and the proposed model also had good performance in predicting the frost resistance of concrete.

6.3. Optimization of Concrete Durability Mix Ratio. The predicted regression functions of frost resistance and permeability indexes are used as the fitness functions. The improved NSGA-II algorithm is used to optimize the multiobjective

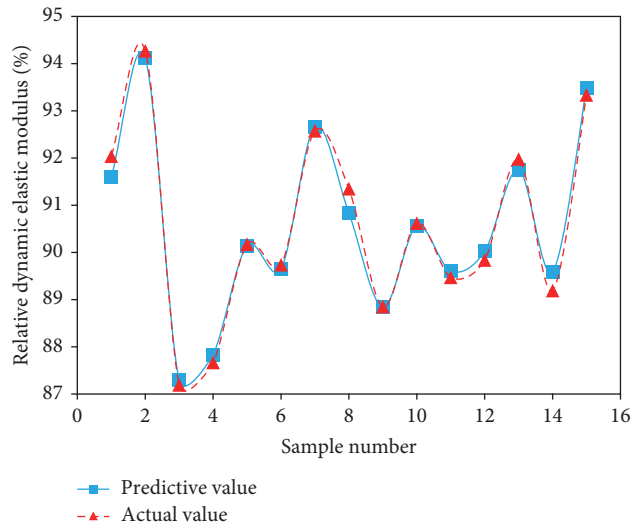

Figure 9: Frost resistance experimental test set prediction results.

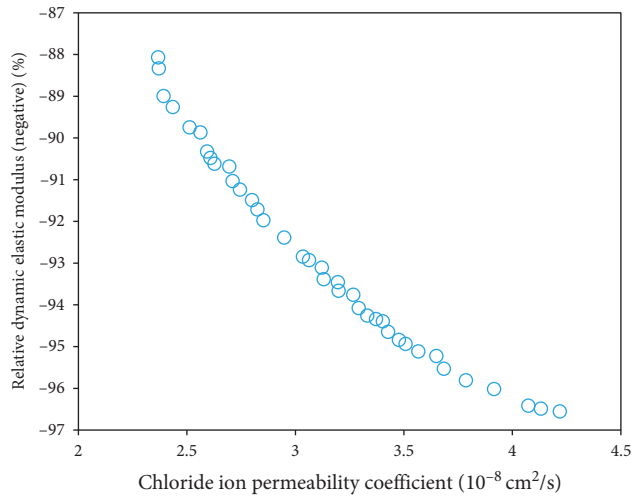

Figure 10: Optimal Pareto frontier.

function, and determine the optimal concrete mix ratio scheme by the ideal point method.

6.3.1. Improving NSGA-II for Multiobjective Optimization. For the improved NSGA-II algorithm, the population type is set to a bidirectional variable. Tent chaotic mapping is introduced to initialize the population, and adaptive crossover operator is used to increase the diversity of the genetic algorithm and avoid falling into the local optimum. The parameters of the algorithm are set as follows: the initial population size is set to 40, the maximum number of genetic generations is set to 60. The crossover probability is set to 0.7, and the variation probability is set to 0.01. The optimal combination of Pareto frontier is obtained after 60 iterations of updating by the multiobjective genetic algorithm, considering that the concrete has good frost and permeability durability, as shown in Figure 10.

Figure 10 gives the image points of the Pareto fronts in the target space obtained by the genetic algorithm after

Table 2: Proportional parameter values corresponding to target optimization results.

No.	x_1	x_2	x_3	x_4	x_5	x_6	x_7	x_8	x_9	x_{10}	F	θ
1	0.375	38.23	373	59.18	770.31	4.92	1144.32	3.53	27.09	0.66	88.03	2.36
2	0.375	38.23	366	59.63	775.93	4.92	1137.65	3.58	27.09	0.65	88.35	2.37
3	0.371	38.07	364	62.72	786.03	5.10	1137.65	3.58	27.06	0.66	89.18	2.42
…	…	…	…	…	…	…	…	…	…	…	…	…
21	0.367	37.55	359	65.77	772.32	5.05	1108.94	3.69	26.97	0.61	93.88	3.10
22	0.365	37.32	357	65.69	772.25	5.03	1109.18	3.69	26.95	0. 62	94.09	3.15
…	…	…	…	…	…	…	…	…	…	…	…	…
36	0.368	37.19	348	66.02	799.45	5.11	1101.25	3.65	26.95	0.67	95.82	4.15
37	0.370	37.19	345	65.38	808.21	4.89	1093.57	3.68	26.99	0.65	96.31	4.19
38	0.370	37.11	345	65.12	810.36	4.89	1093.57	3.68	27.01	0.66	96.59	4.28

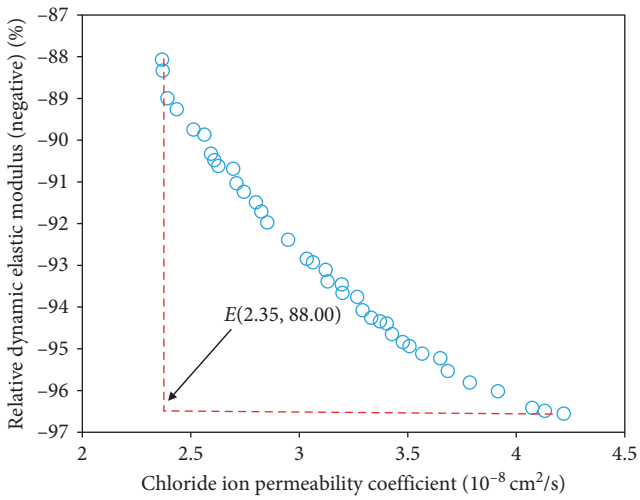

Figure 11: Optimal value ideal point coordinates.

computing the objective function values 2,400 times. The 38 optimization results that satisfy the conditions are calculated based on the prediction model, as shown in Table 2. It can be seen from the figure that the Pareto front is uniformly distributed. The relative dynamic elastic modulus gradually decreases with the decrease of chloride ion permeability coefficient. The minimum chloride ion permeability coefficient can reach 2.36 m^2/s. The corresponding relative kinematic modulus is 88.0%, respectively. The maximum value of relative kinematic modulus is 96.6%. This indicates that the chloride ion permeability coefficient and the relative kinematic modulus are in conflict with each other (Table 2). In the process of moving from the left end to the right end of the optimal Pareto front in the figure, the NSGA-II algorithm nondominated solution moves from the optimal solution for the chloride ion permeability coefficient to the optimal solution for the relative kinetic elastic modulus.

6.3.2. Optimal Pareto Selection. Among the obtained optimal Pareto fronts, there is uniqueness in the optimal solution. In order to obtain the optimal solution, the ideal point method is generally used to determine it, as shown in Figure 11. The optimal value of the chloride permeability coefficient and the relative dynamic elastic modulus constitute the ideal point with the coordinates E (2.35, 88.00). After the ideal point is obtained, the 38 points in the optimal Pareto front are substituted into the ideal point formula, and the optimal solution P (3.15, 94.09) is finally obtained, i.e., the optimal solution is obtained when the chloride ion permeability coefficient is 3.15×10^{-8} cm^2/s and the relative kinetic modulus of elasticity is 94.09%. At this time, the corresponding water/binder ratio is 0.365, and sand rate is 37.32%. The cement content is 357 kg/m^3, and the flyash content is 65.69 kg/m^3. The fine aggregate content is 772.25 kg/m^3, and the nano-SiO_2 content is 5.03 kg/m^3. The coarse aggregate content is 1,109.18 kg/m^3. The water reducer content is 3.69 kg/m^3, and the expansive agent content is 26.95 kg/m^3. The air-entraining agent content is 0.62%.

Based on the optimized parameters, an evaluation model of concrete durability is constructed. It is used to evaluate the relationship between input variables and output variables, to improve the fitting effect between predicted values and actual values, and reduce the matching errors and experimental costs. To verify the accuracy of the proposed algorithm for the multiobjective optimization model of concrete durability, the predicted values under the optimized concrete mix ratio were compared with the experimental values as well as for the comparative analysis in this study are shown in Table 3.

As can be seen from Table 3, the error between the predicted values and the experimental values of chloride ion permeability coefficient and relative dynamic elastic modulus under the optimal mix proportion of concrete is very small. Among them, the predicted value of chloride ion permeability coefficient of the proposed model is 3.15, which is 1.29% different from the actual value of the test. The predicted value of the relative dynamic elastic modulus is 94.09, which is 0.59% different from the real test value. Compared with SVM-NSGA-II, RF-NSGA-II, and LSSVM–NSGA-II, the proposed model has the best prediction performance. The experimental results show that the algorithm proposed in this paper is reliable and accurate in multiobjective optimization of concrete durability, and has good prediction ability and strong generalization ability.

Table 3: Comparison of optimization values for concrete durability.

	Chloride ion permeability chloride ion permeability coefficient (10^{-8} cm^2/s)		Relative dynamic elastic relative dynamic elastic modulus (%)	
	Value	Error (%)	Value	Error (%)
Test value	3.11	–	94.65	–
Proposed algorithm	3.15	1.29	94.09	0.59
SVM-NSGA-II [38]	3.23	3.86	92.68	2.08
RF-NSGA-II [39]	3.19	2.57	93.15	1.58
LSSVM-NSGA-II [40]	3.05	1.93	93.40	1.32

7. Conclusion

(1) The paper proposes a novel method for self-healing concrete using nano-SiO_2 filler to address the issue of common cracks in conventional concrete. This approach effectively improves the strength recovery rate and overall durability of concrete, thereby prolonging the service life of civil infrastructure.

(2) We have constructed an evaluation model based on PSO-LSSVM and an improved NSGA-II algorithm to quickly and accurately determine the optimal design of concrete mix proportions. Ten factors, including water–binder ratio, sand ratio, cement, fly ash, fine aggregate, coarse aggregate, nano-SiO_2, water-reducing agent, expansive agent, and air-entraining agent, are selected as input variables. The evaluation model considers frost resistance and impermeability as the durability optimization objectives. By incorporating constraint conditions related to raw materials and mix proportions, along with specifications and project requirements, we are able to select an optimal durability concrete scheme. Experimental results show that the proposed self-healing concrete scheme effectively resolves mechanical property degradation caused by cracks in conventional concrete, leading to enhanced durability of civil infrastructure. The objective optimization outcomes of the evaluation model align well with engineering practice. The proposed method is an intelligent, accurate, and efficient mix proportion optimization approach, holding significant practical value in engineering production and providing valuable guidance for engineering practice.

(3) To address the issue of the NSGA-II algorithm getting stuck in local optima within the evaluation model, we have proposed an improved NSGA-II algorithm. This enhanced version incorporates Tent chaotic mapping for the population initialization and adopts an adaptive crossover operator, enabling the algorithm to avoid the local optimization pitfalls.

Regarding the sample size of the mix ratio data obtained in this study, we acknowledge that it is relatively small, and it may affect the performance of the evaluation model. In the future, we plan to enhance the prediction optimization effect by obtaining more data. Additionally, we aim to expand the optimization targets to include durability, strength, and economic cost of concrete, considering mix ratio optimization design under more factors.

Data Availability

The labeled data set used to support the findings of this study is available from the corresponding author upon request.

Conflicts of Interest

The authors declare that they have no conflicts of interest.

Acknowledgments

This work is supported by the Huanghe Jiaotong University.

References

[1] X. Zhu, Z. Guo, W. Yang, and W. Song, "Durability of concrete with coal gasification slag and coal gangue powder," *Frontiers in Materials*, vol. 8, Article ID 791178, 2022.

[2] Y. Xu, H. Ye, Q. Yuan, C. Shi, Y. Gao, and Q. Fu, "The durability of concrete subject to mechanical load coupled with freeze–thaw cycles: a review," *Archives of Civil and Mechanical Engineering*, vol. 22, Article ID 47, 2022.

[3] W. L. Baloch, H. Siad, M. Lachemi, and M. Sahmaran, "A review on the durability of concrete-to-concrete bond in recent rehabilitated structures," *Journal of Building Engineering*, vol. 44, Article ID 103315, 2021.

[4] M. R. Hossain, R. Sultana, M. M. Patwary, N. Khunga, P. Sharma, and S. J. Shaker, "Self-healing concrete for sustainable buildings. A review," *Environmental Chemistry Letters*, vol. 20, pp. 1265–1273, 2022.

[5] F. Althoey, M. N. Amin, K. Khan et al., "Machine learning based computational approach for crack width detection of self-healing concrete," *Case Studies in Construction Materials*, vol. 17, Article ID e01610, 2022.

[6] A. AlArab, B. Hamad, and J. J. Assaad, "Strength and durability of concrete containing ceramic waste powder and blast furnace slag," *Journal of Materials in Civil Engineering*, vol. 34, no. 1, Article ID 04021392, 2022.

[7] A. R. Suleiman, L. V. Zhang, and M. L. Nehdi, "Quantifying crack self-healing in concrete with superabsorbent polymers under varying temperature and relative humidity," *Sustainability*, vol. 13, no. 24, Article ID 13999, 2021.

[8] K. Huang, B. J. Wu, K. K. Tang, and Z. X. Li, "Hygro-chemical-mechanical multi-field coupling analysis on damage-healing behavior of concrete," *Chinese Quarterly of Mechanics*, vol. 42, no. 3, pp. 490–497, 2021.

[9] S. Farhadi and S. Ziadloo, "Self-healing microbial concrete—a review," *Materials Science Forum*, vol. 990, pp. 8–12, 2020.
[10] S. I. Zaki, O. A. Hodhod, and M. F. Eid, "Evaluating the effect of using nano bentonite on strength and durability of concrete," *Nano Hybrids and Composites*, vol. 36, pp. 125–141, 2022.
[11] S. L. Miao, Y. M. Zhou, K. Y. Chen, Y. C. Huang, and Y. Y. Sun, "Research progress on the influence of nanomaterials on the performance of concrete," *China Concrete and Cement Products*, vol. 276, no. 4, pp. 20–23, 2019.
[12] F. Geng, Z. Liang, H. Yang, Z. Wu, X. Zhu, and J. Xu, "Effect of silica fume on early performance of precast concrete with early strength agents," *Transactions of Nanjing University of Aeronautics and Astronautics*, vol. 39, no. S1, pp. 90–97, 2022.
[13] K. Cao, Y. Ji, X. Fang et al., "Mix design and performance study of granite manufactured sand concrete with different stone powder content," *Concrete*, vol. 402, no. 4, pp. 120–125 130, 2023.
[14] J. Tu, Y. Liu, M. Zhou, and R. Li, "Prediction and analysis of compressive strength of recycled aggregate thermal insulation concrete based on GA-BP optimization network," *Journal of Engineering, Design and Technology*, vol. 19, no. 2, pp. 412–422, 2021.
[15] N.-J. Wu, "Predicting the compressive strength of concrete using an RBF-ANN model," *Applied Sciences*, vol. 11, no. 14, Article ID 6382, 2021.
[16] N. Abunassar, M. Alas, and S. I. A. Ali, "Prediction of compressive strength in self-compacting concrete containing fly ash and silica fume using ANN and SVM," *Arabian Journal for Science and Engineering*, vol. 48, pp. 5171–5184, 2023.
[17] M. Kumar, V. Kumar, R. Biswas et al., "Hybrid ELM and MARS-based prediction model for bearing capacity of shallow foundation," *Processes*, vol. 10, no. 5, Article ID 1013, 2022.
[18] D. R. Kumar, P. Samui, and A. Burman, "Prediction of probability of liquefaction using hybrid ANN with optimization techniques," *Arabian Journal of Geosciences*, vol. 15, Article ID 1587, 2022.
[19] R. Biswas, M. Kumar, R. K. Singh et al., "A novel integrated approach of RUNge Kutta optimizer and ANN for estimating compressive strength of self-compacting concrete," *Case Studies in Construction Materials*, vol. 18, Article ID e02163, 2023.
[20] P. Zhang, C. D. Li, J. Wang, and L. Y. Kang, "Mechanical properties of concrete synergistically reinforced with Nano-SiO2 and polyvinyl alcohol fiber," *Highway*, vol. 66, no. 2, pp. 271–275, 2021.
[21] R. Abousnina, A. Manalo, W. Ferdous, W. Lokuge, B. Benabed, and K. S. Al-Jabri, "Characteristics, strength development and microstructure of cement mortar containing oil-contaminated sand," *Construction and Building Materials*, vol. 252, Article ID 119155, 2020.
[22] M. Stefanidou, E. Tsampali, G. Karagiannis, S. Amanatiadis, A. Ioakim, and S. Kassavetis, "Techniques for recording self-healing efficiency and characterizing the healing products in cementitious materials," *Material Design & Processing Communications*, vol. 3, no. 3, Article ID e166, 2021.
[23] M. Stefanidou, E.-C. Tsardaka, and A. Karozou, "The influence of curing regimes in self-healing of nano-modified cement pastes," *Materials*, vol. 13, no. 22, Article ID 5301, 2020.
[24] M. Gohar, F. Ali, I. Khan, N. A. Sheikh, and A. Shah, "The unsteady flow of generalized hybrid nanofluids: applications in cementitious materials," *Journal of the Australian Ceramic Society*, vol. 55, pp. 657–666, 2019.
[25] M. Rajasegar and C. Manoj Kumaar, "Hybrid effect of poly vinyl alcohol, expansive minerals, nano-silica and rice husk ash on the self-healing ability of concrete," *Materials Today: Proceedings*, vol. 45, Part 7, pp. 5944–5952, 2021.
[26] T. Evangelia and S. Maria, "Effect of nano-SiO_2 and nano-CaO in autogenous self-healing efficiency," *Materials Today: Proceedings*, vol. 37, Part 4, pp. 4071–4077, 2021.
[27] R. Wang, Z. Hu, Y. Li, K. Wang, and H. Zhang, "Review on the deterioration and approaches to enhance the durability of concrete in the freeze–thaw environment," *Construction and Building Materials*, vol. 321, Article ID 126371, 2022.
[28] R. He, T. Wang, H. X. Chen, C. Xu, and Y. H. Bai, "Impact of qinghai–tibet plateau's climate on strength and permeability of concrete," *China Journal of Highway and Transport*, vol. 33, no. 7, pp. 29–41, 2020.
[29] Y. C. Guo, Z. H. Chen, A. Q. Shen, and P. Li, "Optimization mix design of bridge deck concrete based on crack resistance in alpine regions," *Journal of Chang'an University (Natural Science Edition)*, vol. 39, no. 4, pp. 1–8, 2019.
[30] W. Gong, H.-F. Yu, H.-Y. Ma, N. Wang, and H.-W. Zhu, "Durability of concrete with different improvement measures and its service life prediction in island and reef environment," *China Ocean Engineering*, vol. 36, pp. 947–958, 2022.
[31] M. B. Leite and V. M. Santana, "Evaluation of an experimental mix proportion study and production of concrete using fine recycled aggregate," *Journal of Building Engineering*, vol. 21, pp. 243–253, 2019.
[32] C. Xu, W. Ni, K. Li, S. Zhang, Y. Li, and D. Xu, "Hydration mechanism and orthogonal optimisation of mix proportion for steel slag–slag-based clinker-free prefabricated concrete," *Construction and Building Materials*, vol. 228, Article ID 117036, 2019.
[33] J. Zhang, Y. Huang, Y. Wang, and G. Ma, "Multi-objective optimization of concrete mixture proportions using machine learning and metaheuristic algorithms," *Construction and Building Materials*, vol. 253, Article ID 119208, 2020.
[34] Y. Huang, J. Zhang, F. T. Ann, and G. Ma, "Intelligent mixture design of steel fibre reinforced concrete using a support vector regression and firefly algorithm based multi-objective optimization model," *Construction and Building Materials*, vol. 260, Article ID 120457, 2020.
[35] X. Xue, "Evaluation of concrete compressive strength based on an improved PSO-LSSVM model," *Computers and Concrete, An International Journal*, vol. 21, no. 5, pp. 505–511, 2018.
[36] B. Han, J. Wang, S. Li, and J. Zhang, "Study on multi-objective optimization of wet sprayed concrete parameters based on BP-NSGAII model," *Mining Research and Development*, vol. 42, no. 5, pp. 173–178, 2022.
[37] Y. Liu, Y. Cao, L. Wang, Z.-S. Chen, and Y. Qin, "Prediction of the durability of high-performance concrete using an integrated RF-LSSVM model," *Construction and Building Materials*, vol. 356, Article ID 129232, 2022.
[38] F. C. Liu, T. T. Deng, C. L. Wang et al., "Multi-objective optimization of durability concrete mix ratio based on SVM-NSGAII," *Journal of Civil Engineering and Management*, vol. 37, no. 6, pp. 86–92 100, 2020.
[39] X. Wu, L. Wang, H. Chen, Z. Feng, Y. Qin, and W. Xu, "Multi-objective optimization of high-performance concrete durability mix ratio based on RF-NSGA II," *Materials Reports*, vol. 36, no. 17, Article ID 20110015-7, 2022.
[40] H. Chen, T. Deng, T. Du, B. Chen, M. J. Skibniewski, and L. Zhang, "An RF and LSSVM–NSGA-II method for the multi-objective optimization of high-performance concrete durability," *Cement and Concrete Composites*, vol. 129, Article ID 104446, 2022.